



# University of HUDDERSFIELD

## University of Huddersfield Repository

Jiang, Xiangqian, Abdul-Rahman, Hussein S. and Scott, Paul J.

Multi-scale freeform surface texture filtering using a mesh relaxation scheme

### Original Citation

Jiang, Xiangqian, Abdul-Rahman, Hussein S. and Scott, Paul J. (2013) Multi-scale freeform surface texture filtering using a mesh relaxation scheme. *Measurement Science and Technology*, 24 (11). ISSN 0957-0233

This version is available at <http://eprints.hud.ac.uk/18562/>

The University Repository is a digital collection of the research output of the University, available on Open Access. Copyright and Moral Rights for the items on this site are retained by the individual author and/or other copyright owners. Users may access full items free of charge; copies of full text items generally can be reproduced, displayed or performed and given to third parties in any format or medium for personal research or study, educational or not-for-profit purposes without prior permission or charge, provided:

- The authors, title and full bibliographic details is credited in any copy;
- A hyperlink and/or URL is included for the original metadata page; and
- The content is not changed in any way.

For more information, including our policy and submission procedure, please contact the Repository Team at: [E.mailbox@hud.ac.uk](mailto:E.mailbox@hud.ac.uk).

<http://eprints.hud.ac.uk/>

# Multi-Scale Freeform Surface Texture Filtering using a Mesh Relaxation Scheme

Xiangqian (Jane) Jiang<sup>1</sup>, Hussein S. Abdul-Rahman<sup>1</sup> and Paul J. Scott<sup>1</sup>

[x.jiang@hud.ac.uk](mailto:x.jiang@hud.ac.uk), [h.abdul-rahman@hud.ac.uk](mailto:h.abdul-rahman@hud.ac.uk), [p.j.scott@hud.ac.uk](mailto:p.j.scott@hud.ac.uk)

<sup>1</sup>*EPSRC Centre for Innovative Manufacturing in Advanced Metrology, Centre for Precision Technologies, School of Computing and Engineering, University of Huddersfield, Huddersfield HD1 3DH, UK.*

## Abstract

Surface filtering algorithms using Fourier, Gaussian, wavelets ... etc., are well-established for simple Euclidean geometries. However, these filtration techniques cannot be applied to today's complex freeform surfaces, which have non-Euclidean geometries, without distortion of the results. This paper proposes a new multi-scale filtering algorithm for freeform surfaces that are represented by triangular meshes based on a mesh relaxation scheme. The proposed algorithm is capable of decomposing a freeform surface into different scales and to separate surface roughness, waviness and form from each other as will be demonstrated throughout the paper. Results of applying the proposed algorithm to computer-generated as well as real surfaces are represented and compared with a lifting wavelet filtering algorithm.

**Keywords:** Freeform surfaces; filtering; mesh relaxation; multi-scale analysis; surface metrology.

## 1- Introduction

Surface is an important feature of manufactured engineering products: it provides the functional interface through which these products operate and interact with the environment and with each other. The performance of the manufactured workpiece depends on the quality of the manufactured surface and on the ability to measure and assess that quality. Surface metrology is the science that offers the tools for analysing and assessing the quality of these surfaces.

Surface metrology can be defined as the measurement and characterisation of the deviations of a workpiece from its intended shape [1]. These deviations are usually classified according to their wavelengths (scales) into three types of irregularities namely; roughness, waviness and form.

Roughness and waviness are usually grouped together under the general term of surface texture.

Measuring and characterising ordinary simple surfaces such as planes, spheres and cylinders is mature and has been intensively studied and developed [1-6]. Many research papers and industrial standards have been published describing the measurement and characterisation of such simple surfaces [4-11]. However, with the development of science and technology, more and more complex surfaces are being produced which, unlike the conventional surfaces, have no axes of rotation and no translational symmetry and could have any shape or design; such complex surfaces have been termed “freeform surfaces”.

The characterisation and parameterisation of surface texture can be divided into four major steps namely: surface sampling and representation; decomposition and filtration; texture representation and mapping; and finally characterisation and parameterisation as shown in Fig. 1. All four steps are required before a full analysis of surface texture is possible. Each of these steps has been heavily investigated and it is now well established over simple geometries. However, moving from simple geometries to complex freeform geometries is challenging; many of the traditional techniques that have been used to perform these tasks, shown in Fig. 1, start to fail. Therefore, new theories and tools that can cope with the new emerging freeform surfaces are required.

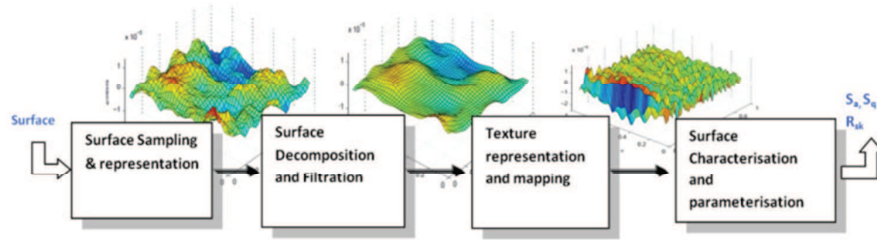


**Fig. 1:** Texture characterisation and parameterisation process

Surface decomposition and filtration is an essential step in the texture characterisation process. During the last decade, decomposition and filtration techniques for simple surfaces have been comprehensively investigated and many algorithms based on Fourier, Gaussian, Spline and wavelet techniques were proposed and became the industrial filtration standards [7-11]. Unfortunately, all of these techniques are designed to decompose and filter Euclidean surfaces, so most of these techniques fail to filter freeform non-Euclidean surfaces.

Recently, new filtering algorithms based on discrete modal decomposition have been proposed [12, 13]. In these techniques, the measured surface is decomposed using a family of a discrete functions, called modes or modal deformations, and therefore the measured surface can be represented as a combinations of these modes with different amplitudes. The filtering in such algorithms is carried out by reconstructing the surface using some of the surface modes. Theoretically, this method is valid for different type of surfaces. The results of the applying this method to filter surfaces represented on a regular grid are shown in [12, 13].

In the past two years, our research group have proposed three novel filtration techniques that are capable of filtering freeform non-Euclidean surfaces represented by triangular meshes. The first technique is based on solving the diffusion equation formulated by using the Laplace-Beltrami operator on that surface [14]. The second algorithm is based on using morphological operations [15]. The third method is based on a generalised lifting wavelet transform [16].

In this paper, a new filtering method is proposed that is capable of filtering freeform non-Euclidean surfaces represented by triangular meshes based on a mesh relaxation scheme. This work is part of an on-going research programme into surface texture analysis for complex freeform surfaces and represents an investigation into filtration of complex freeform surfaces only. The proposed algorithm is capable of decomposing freeform surface into different scales, i.e. roughness, waviness and form. This paper provides the initial investigations of applying a mesh relaxation scheme for freeform surface filtration. The power of this filtration technique is that it is capable of filtering any type of freeform surfaces represented by a triangular mesh as will be discussed and presented in the paper.

This paper is organised as follows: section 2 discusses the difference between Euclidean and freeform non-Euclidean surfaces and also explains why new algorithms are needed to handle freeform surfaces; section 3 previews different methods of representing freeform surfaces; a brief review of existing multi-scale analysis methods for surfaces represented by triangular meshes is shown in section 4; section 5 details the proposed multi-scale mesh relaxation filtering algorithm; section 6 shows the results of applying the proposed algorithm to simulated and real measured data and also compares the results with a lifting based filtering algorithm; and finally the conclusions and future work are discussed in section 7.

## **2- The need of new filtering methods for freeform surfaces**

In simple geometries, surfaces are regarded as a continuous function that defines a height value over a planar domain. Each point of this domain defines a single height value of the surface. This planar domain have zero curvature everywhere therefore is called Euclidean domain and consequently such simple surfaces are called Euclidean surfaces. Furthermore, Euclidean surfaces can be projected onto a plane without causing any distortion or loss of surface information, therefore such surfaces are usually represented as a height values over a regular 2D grid.

Freeform surfaces have a more complex nature. The underlying domain is no longer a plane and contains points that have non-zero curvature therefore is called non-Euclidean; such freeform surfaces are also called non-Euclidean surfaces. According to Gauss's theorem in differential geometry,

Theorema Egregium, surfaces with the same curvature can be mapped into each other without any distortion, for example surfaces with zero-curvature like planes, cylinders and cones can be transformed into each other without any distortion. In contrast, Surfaces with different curvature cannot be mapped into each other without distortion, for example, the Earth cannot be displayed on a planner map without distortion [17]. Subsequently, freeform non-Euclidean surface cannot be projected onto a plane without distortion or loss of some surface information. As a result, freeform surfaces can no longer be represented as a height values over a two dimensional grid. For example, if attempts are made to represent a hemisphere surface over 2D grid, this will cause a distortion of the geodesic distances on the surface, i.e. the geodesic distances between different points on the actual surface will be distorted and will be smaller when projected onto the 2D grid. The geodesic distance between two points on a given surface is defined as the shortest path between the two points on that surface. Another example showing the invalidity of representing freeform non-Euclidean surfaces using 2D grid is that the lack of such method to represent closed surfaces such as a sphere.

Most well-established surface filtering methods and operations such as; Fourier analysis, first generation wavelets decompositions, Gaussian filters, linear and robust filters, Spline filters and convolution operations, are theoretically valid only for Euclidean geometries that have no curvature and are not immediately applicable on non-Euclidean geometries. Applying these methods for filtering freeform non-Euclidean surface will reduce the accuracy of the filtering results which will consequently will give a misleading indication of the quality of that surface. Therefore, it is important to investigate the extension of these filtering techniques and also to come up with new techniques to handle non-Euclidean freeform surfaces that can no longer be represented as height values over 2D grids. These new methods will give a more accurate indication of the quality of these surfaces and therefore improve their functional performance.

### **3- Representation of freeform surfaces**

There are a number of techniques that can be used to represent freeform surfaces. Most of these techniques originated in the field of computer graphics and can be roughly classified into two major

categories namely; the discrete methods and the continuous methods. A survey of surface representation techniques can be found in [18].

Continuous representation methods attempt to reconstruct the continuous surface from the discrete measurement points. Reconstructing the continuous surface is not a trivial task as it requires finding an equation or a set of equations that would approximate the surface up to a certain degree. B-SPLINES and radial basis functions (RBFs) are examples of the continuous methods [19, 20].

The discrete representation consists mainly of two major types; point clouds and polygon surface meshes. Point clouds are a primitive way of representing a surface, as they only store the surface as a number of  $(x,y,z)$  coordinates and no geometrical properties can be obtained from this type of presentation. Surface meshes, on the other hand, have been widely used in representing surfaces in many different fields for many reasons; for example: representation of surfaces of different topological types; geometrical approximations and also they are easier to implement than other surface representation types. Surface meshes, in particular triangular meshes, are adopted to represent the freeform surfaces presented in this paper.

A triangular mesh can be simply defined as a collection of vertices (points), edges and faces that define the shape or a surface of a 3D object. Three major types of meshes according to the distribution of the vertices, edges and faces among the entire surface can be distinguished; regular, semi-regular and irregular meshes, as shown in Fig. 2 [21].

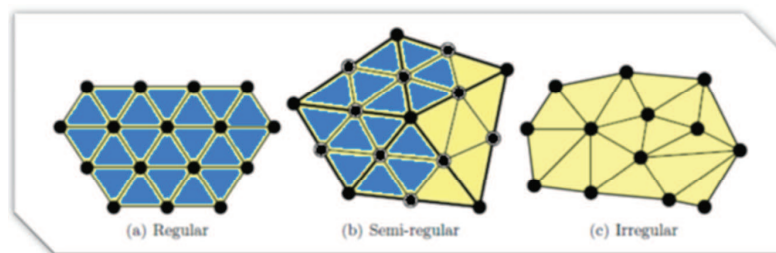


**Fig. 2:** Different types of triangular meshes: (a) regular, (b) semi-regular and (c) irregular

Regular mesh is a type of mesh where its vertices are regularly distributed among the entire surface, all the faces have almost the same area and all vertices have the same number of edges. Semi-regular mesh is a mesh that is considered to be regular on local areas but not on the entire surface. Irregular mesh is a mesh which does not possess any of the properties above, the area of each face (triangle) is different to each other, and also the number of edges per vertex varies [21].

Most of regular and semi-regular types of meshes can be found in computer graphics and computer generated surfaces, however they are not commonly found in actual measured surfaces. Irregular type meshes are more realistic and suitable from a surface texture point of view than the other two types; this is why the proposed algorithm targets freeform surfaces that are represented by irregular meshes.

#### **4- Multi-scales analysis on surfaces represented by triangular meshes: a review**

Multi-scale or Multi-resolution analysis (MRA) for 3D triangular meshes has been an active research area for the past decade. The main idea behind MRA is to split a high resolution mesh into a lower resolution or a smoother mesh, which usually refer to as the approximation, and the details that are needed to recover the original mesh. This operation of splitting can be repeated for many levels, where each level represents a different scale.

The introduction of the second generation wavelets and lifting scheme [22-24] made the extension of wavelets and MRA possible for irregular data sets and for different types of 3D meshes and graphs and a few algorithms have been proposed [21, 25-33].

Lounsbery *et al.* have proposed a bi-orthogonal filter banks to decompose a regular and semi-regular 3D meshes into a lower resolution counterpart and a series of wavelets coefficients as shown in Fig. 3. In their method, they made the connection between the nested spaces of scaling functions and 3D mesh decomposition through the subdivision operation. They show that the subdivision scheme can be used to create the nested linear spaces required to build the MRA [26]. The decomposition is computed with two analysis filters,  $A^j$  and  $B^j$  for each resolution level  $j$ . The reconstruction is carried out with two synthesis filters  $P^j$  and  $O^j$ . They showed that a coarser mesh and its wavelet coefficients ( $V^j$  and  $W^j$  respectively) can be calculated from a finer mesh  $V^{j+1}$  using the following equations:



$$V^j = A^j V^{j+1} \quad (1)$$

$$W^j = B^j V^{j+1} \quad (2)$$

The finer mesh  $V^{j+1}$  can be recovered from its coarser approximation and wavelets coefficients using a pair of synthesis filters  $P^j$  and  $Q^j$ ;

$$V^{j+1} = P^j V^j + Q^j W^j \quad (3)$$

Where the connection between the analysis and synthesis filters that insures a perfect reconstruction is given by:

$$\begin{bmatrix} A^j \\ B^j \end{bmatrix} = [P^j \quad Q^j]^{-1} \quad (4)$$

This technique works only on regular and semi-regular meshes with subdivision connectivity but fails to handle the irregular cases.

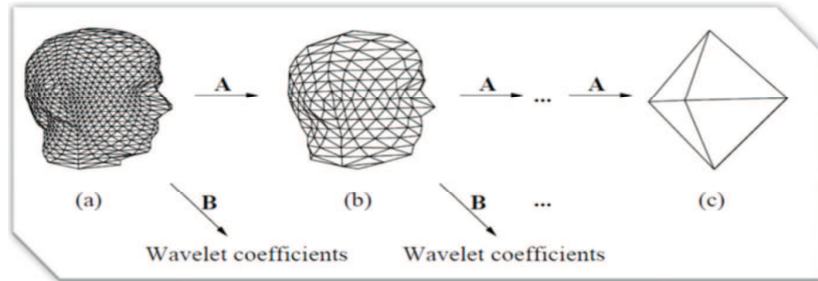


**Fig.3:** Decomposition of 3D mesh into approximation and details as proposed by Lounsbery[26].

Bonneau introduced multi-resolution analysis over non-nested spaces using what he called BLac-wavelets. BLac-wavelet is a combination of the Haar function with the linear B-Spline function. In his work two major operators were proposed: the smoothing operator to compute the coarse mesh; and an error operator to determine the difference between the approximation and the original meshes [27].

Daubechies *et al.* proposed another technique that can handle irregular 3D meshes. Their technique is based on mesh simplification and subdivision schemes, the authors use a Burt-Adelson pyramid

scheme as shown in Fig.4. The design of the subdivision scheme is carried out by inserting new values in such a manner that the second order differences are minimized [28].

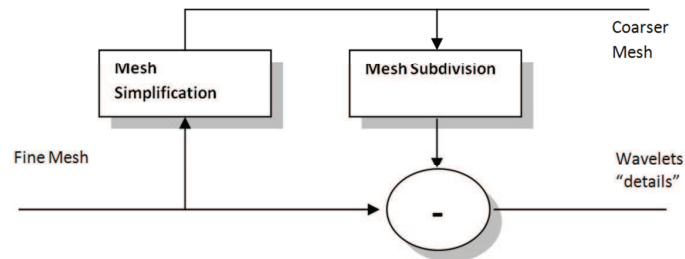


**Fig.4:** Decomposition of irregular 3D meshes using a Burt-Adelson pyramid-like scheme.

Other researchers proposed the use of the lifting scheme to decompose the surfaces. Schroder and Swelden have proposed an extension of the lifting scheme to decompose spherical surfaces [32, 33]. Roy *et al.* have proposed a MRA for irregular meshes based on split and predict operations [29]. This algorithm consists of three main steps: split, predict and down-sampling. The split operator separates the odd and even vertices. The odd vertices were defined as a set of independent vertices which are not directly connected by an edge. All the selected odd vertices are removed by a mesh simplification algorithm in the global down-sampling stage, and then predicted back using the prediction operator that relax the curvature based on the Meyer smoothing operator [34,35]. Szczensa proposed a new multi-resolution analysis for irregular meshes using the lifting scheme, in which she proposed a new prediction operator using Voronoi cells in a local neighbourhood [36, 37]. Very recently, the authors have proposed a lifting based algorithm to filter the texture on freeform surface, this technique consisted of five major operators; split, predict, update, simplify (down-sampling) and merge (up-sampling) [16].

Valette *et al.* presented a wavelet-based multi-resolution decomposition of irregular surface meshes. The method is essentially based on Lounsbery decompositions. However they introduced a new irregular subdivision scheme and a complex simplification technique in order to define surface

patches suitable for the irregular meshes [38]. A review of recent advances in multiresolution analysis for 3D meshes can be found in [39].

### 5- Freeform surface texture filtering using mesh relaxation schemes

Filtering a regular 1D or 2D signal in time/spatial domain is usually carried out by defining a weighted 1D or 2D window, usually referred to as the kernel. This weighted kernel is used to calculate a weighted summation that represents a new functional or attribute value at a certain data position, and then it is translated across the signal to calculate the new values at other positions. The weights inside the kernel are assigned using many different methods depending on the application, for example, the weights could represent a Gaussian filter, Laplacian coefficients, Sobel coefficients.

In an analogy with regular cases, mesh relaxation could be defined as the extension of the weighted window (kernel) to the irregular cases. In other words, mesh relaxation is the process of calculating a new function value at a particular position of the mesh based on a weighted kernel defined by the mesh relaxation scheme, as shown in Fig.5. In Fig. 5(a), the central vertex of the mesh, that has the value of 6, is to be relaxed using the weighted kernel which is represented by smaller circles, applying this kernel will result of new relaxed value of 5.7 that would replace the original value as shown in Fig. 5(b). Unlike the regular cases, the kernel in the irregular data sets has to be adaptive in the size (number of kernel nodes) and the weights. These two parameters have to be continuously changing depending on geometry and/or connectivity between the data points at each vertex of the mesh.

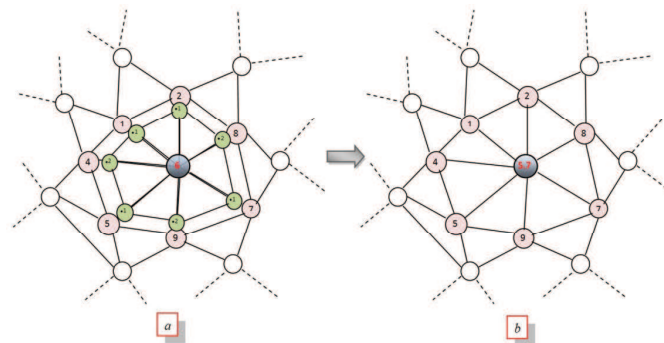


**Fig.5:** Demonstration of mesh relaxation using a mesh kernel: (a) the original mesh and the kernel associated with the centre vertex; (b) the relaxed value of the centre vertex calculated using the kernel.

Mesh relaxation plays an important role in building a multi-resolution analysis for 3D triangular meshes. Guskov *et al.* (1999) were the first to propose a multi-resolution signal processing tool for 3D triangular meshes with a mesh relaxation operator being the central ingredient in the algorithm [21]. They proposed a non-uniform relaxation operator that minimizes the second order differences (SOD) at every edge of the mesh.

Roy *et al.* proposed another mesh relaxation algorithm to build a multi-resolution analysis for irregular 3D meshes based on a non-uniform relaxation operator that minimizes the local curvature of the mesh [29, 40]. Roy's curvature relaxation was inspired by the work of Meyer *et al.* [35] on the local and accurate discrete differential-geometry operators which was previously applied for surface de-noising [34, 41].

The two relaxation scheme were compared [40, 42] and comparisons showed that the two relaxation operators gives similar smoothing results. However, the curvature relaxation is four times faster than the SOD operator [40]. The SOD relaxation uses the 2-ring neighbourhood to compute a new relaxed value of the mesh whereas the curvature relaxation requires only the 1-ring neighbourhood. The 1-ring neighbourhood of a vertex  $v$  is defined as the set of vertices that are only one edge away from that vertex  $v$ . The 2-ring neighbourhood is defined as the set of vertices that are less than 2 edges away from the vertex  $v$ . An example of 1-ring and 2-ring neighbours is shown in Fig. 6.

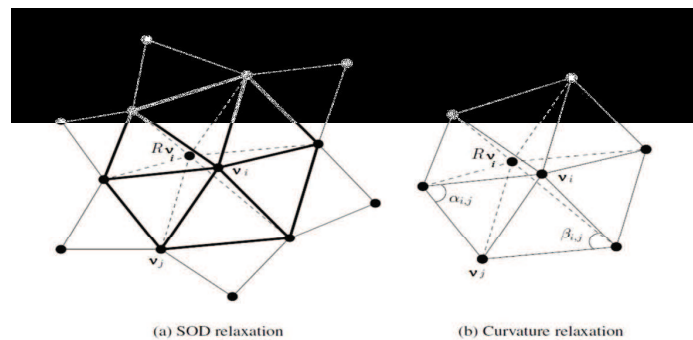


**Fig.6:** Example of 1-ring and 2-ring neighbours of a vertex  $v$ ; (a) the 2-ring neighbourhood used in the SOD relaxation scheme; (b) the 1-ring neighbourhood used in the curvature relaxation scheme.

In this paper the curvature relaxation is adopted to build the multi-scale filtering technique as explained in the following subsections.

### 5.1. Mesh curvature relaxation

The curvature relaxation operator defines the new function or attribute value of a particular vertex of the mesh based on the Meyer differential operator that minimizes the local curvature of that mesh at a that particular position[35]. The function defined over the mesh could represent any of the attributes associated to that mesh, for example, this function might represent the position of mesh vertices, a colour attribute of each vertex in the mesh for computer graphics applications or, as in this paper, it might represent the surface texture height values associated with mesh vertices from surface metrology point of view.

The relaxed function value  $\mathcal{R}f(v_i)$  of the vertex  $v_i$  using the curvature relaxation operator is given by:

$$\mathcal{R}f(v_i) = \sum_{j \in \mathcal{N}_1(v_i)} w_{i,j} \cdot f(v_j) \quad (5)$$

Where  $f(v_i)$  could be any function or attribute defined over the vertex  $v_i$ , here it represents the surface texture,  $\mathcal{N}_1(v_i)$  represents the 1-ring neighbourhood of the vertex  $v_i$ ,  $w_{i,j}$  represents the weights of the kernel associated with the vertex  $v_i$  and are defined by:

$$w_{i,j} = \frac{\cot(\alpha_{i,j}) + \cot(\beta_{i,j})}{\sum_{l \in \mathcal{N}_1(v_i)} \{\cot(\alpha_{i,l}) + \cot(\beta_{i,l})\}} \quad (6)$$

The weights  $w_{i,j}$  of the relaxation operator minimises the curvature energy of an edge  $e_{i,j}$  where  $\alpha_{i,j}$  and  $\beta_{i,l}$  are the angles opposite to the edge  $e_{i,j}$  as shown in the Fig. 7. Once the weights are calculated, the new relaxed value can be computed as demonstrated in example shown in Fig.5.

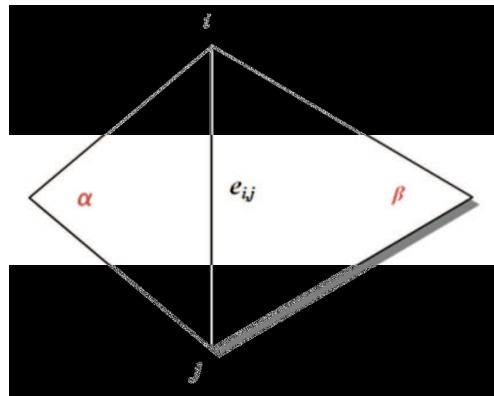


**Fig.7:** The relaxation angles  $\alpha$  and  $\beta$  associated to the edge  $e_{ij}$ .

## 5.2. Multi-scale surface texture filtering using a relaxation scheme.

It is well known that the manufacture of surfaces leaves multi-scale fingerprints within the surface. A manufactured surface will contain three different scales of irregularities which together represent the surface as discussed in the introduction of the paper; the short-scale texture (roughness) which includes tool marks and machine vibrations, the middle-scale texture (waviness) which results from the low variation of the machine, the long-scale (form) which represents the nominal surface form. Decomposing the surface into these different scales is important to characterise and parameterise the surface. Decomposing a freeform surface can be achieved using multiple levels of the mesh curvature relaxation scheme described in the previous section. Each decomposition level contains a mesh relaxation operator that smooths the mesh and a difference operator that calculates the difference between the smoothed and original meshes as shown in Fig. 8. The mesh relaxation operator acts like a low pass smoothing filter and the difference operator acts like a high pass filter which makes this technique similar in concept to the wavelet transform.

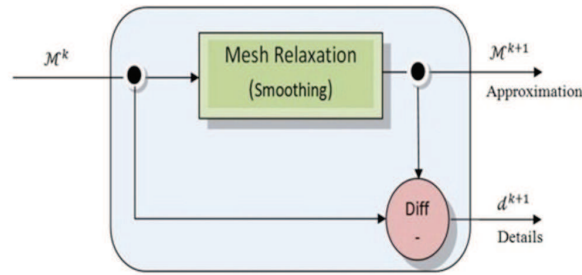


**Fig.8:** One decomposition level of a mesh relaxation scheme.

Decomposing a freeform surface is carried out using a multiple levels of mesh relaxation as shown in Fig.9. The input of first decomposition level of this decomposition ladder is the original surface, represented by triangular mesh, and the two outputs are; a smoother version of the input mesh (the approximation), and also the details coefficients that represent the difference between the input and the approximated mesh (the details). The details are necessary to reconstruct the input surface from its approximation. Each subsequent level consists of further splitting of the smooth (approximated) surface into new two components, namely the approximation which will be even smoother than the input and the details which contain information about the difference between the two levels (the input and output levels) as shown in the Fig. 9. The approximation output at each level becomes the input of the next level and so on. Each level of this decomposition ladder represents a different scale of the original input surface.

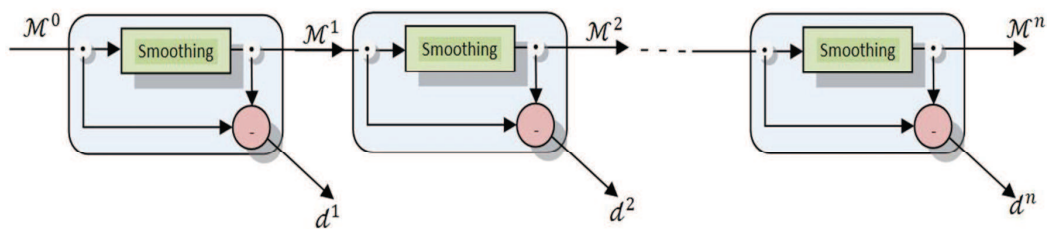


**Fig.9:** Multiple decomposition levels of a mesh relaxation scheme.

The original input mesh can be perfectly reconstructed by adding all of the details to the final approximation output of the final decomposition level  $\mathcal{M}^n$ . The reconstruction can be described mathematically as:

$$\mathcal{M}^0 = \mathcal{M}^n + \sum_{i=0}^n d^i \quad (7)$$

To obtain different scale components of the surface (i.e. roughness, waviness and form), all that is necessary is to set the details coefficients of some levels to zero and then reconstruct the surface using equation 7. By setting the details of some level to zero, the reconstructed surface will consist of only the required scales and will filter out all other scales as explained in the next subsection.

### 5.3- Scale-limited surfaces using mesh relaxation

The concept of scale-limited surfaces was introduced by Jiang *et al.* for areal surface texture [5, 11, 43]. Scale-limited surfaces provides a flexible way to identify various different scales of surface texture. Instead of characterising the surface using the traditional parameters; the form, waviness and roughness, the surface is now characterised using a different filters and operators that decompose the surface into three main scales namely; the short-scale surface (SL surface), the middle-scale surface (SF surface) and the long-scale form surface (F-operator) as shown in Fig. 10, these different scales are equivalent to the roughness, waviness and the form in the traditional definitions.



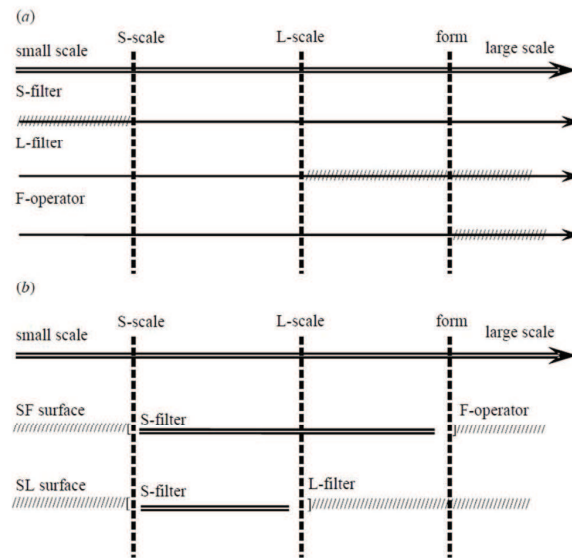


**Fig.10:**The concept of the scale-limited surfaces: (a) Filters and operators used in Surface texture; (b) Scale-limited surface used in surface texture.

Obtaining different scale-limited surfaces using the mesh relaxation scheme is explained with the help of Fig. 11. Fig.11(a) shows a spectral-like decomposition of a freeform surface using an decomposition levels. As shown in the figure, the surface can be represented using the smoothest approximation and a series of the details coefficients from all decomposition levels as explained mathematically in the Eq. 7. Lower indices in the figure represent smaller scales and higher indices represent longer scales.

The long-scale form surface can be extracted by selecting the smoothest approximation, and the details of some higher indexed levels, and filtering out all other levels. This operation is equivalent to a low pass filtering of the given spectrum. The middle-scale surface can be extracted by choosing the details of some of the middle levels which is equivalent to a band pass filtering of the spectrum. The short-scale surface is extracted by choosing the details of lower indexed levels which is considered as a high pass filtering of the spectrum. The extraction of these different scale-limited surfaces is shown in Fig. 11(b).

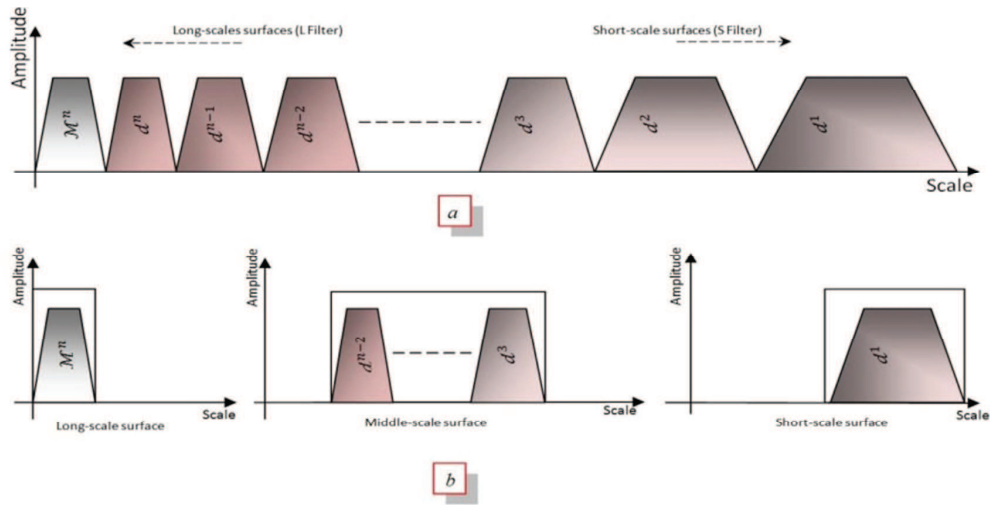


**Fig.11:**Spectral-like analysis of a freeform surface using mesh relaxation scheme: (a) spectral-like analysis of a freeform surface; (b) the extraction of different scale-limited surfaces: (right) the long-scale surface extracted using low pass filtering of the spectrum; (middle) the middle-scale surface extracted by band pass filtering; (left) the short-scale surface extracted using high pass filtering.

## 6- Results and Discussions

The aforementioned algorithm has been implemented and tested to filter and decompose measured and simulated surfaces, represented by 3D irregular triangular meshes, into different components; the results are shown and discussed in this section. Moreover, the proposed technique has been compared with a lifting based filtering approach that splits the surface points into even and odd vertices and then predicts the odd vertices from the even ones as described in [16].

### 6.1- Simulated Surfaces

In order to test the performance of the proposed algorithm to decompose different types of freeform surfaces; three computer generated freeform surfaces are used. These surfaces are designed to cover a wide range of freeform non-Euclidean surfaces with different topological types. The first surface is a saddle shaped surface which is considered to be a typical example of non-Euclidean surface with negative curvature. The second surface is a sphere which represents a positive curvature non-

Euclidean geometry. The third surface is more complicated surface with non-constant curvatures to simulate a complex freeform surface; we refer to this surface as an egg-box surface. All of these surfaces are shown in Fig.12. These surfaces are represented by triangular meshes and the number of faces and vertices for each of these surfaces is shown in Table 1.

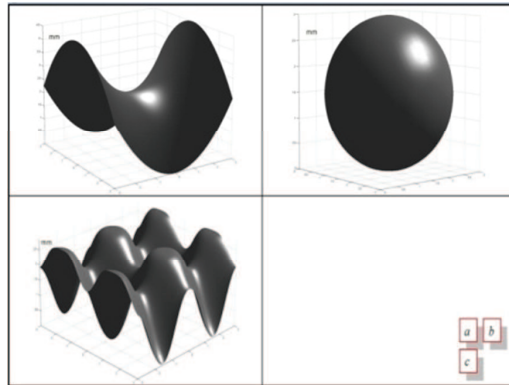


**Fig.12:** Computer generated freeform non-Euclidean surfaces with: (a) negative curvature surface “saddle-shaped surface”; (b) positive curvature surface “spherical surface”; (c) non-constant curvature surface “egg-box surface”.

**Table 1.** Mesh details of the computer generated surfaces

Surface	Faces	Vertices
Saddle-shaped	28800	14641
Sphere	4608	2306
Egg-box surface	28800	14641

To demonstrate the ability of the proposed algorithm to decompose freeform surfaces into different components, an artificial multi-scale texture has been imposed into each of these surfaces. The texture is generated by adding two scale components to surface’s form; the first is a high varying artificial Gaussian noise representing the short-scale texture or surface roughness, and the second is a low

varying sinusoidal surface that would represent the middle-scale texture or surface waviness. The results of applying our technique to these surfaces are shown in Figs. 13 to 15.

Fig. 13 shows the decomposition results of applying the proposed algorithm on the saddle shaped surface. The original textured surface is shown in Fig. 13 (a). Three different components can be easily distinguished in the textured surface: the nominal surface or form surface; the middle-scale surface or surface waviness; and finally the short-scale surface or the surface roughness. The proposed technique has been applied to decompose this surface into its basic components and it successfully manages to disintegrate this surface into different components as shown in Figs. 13(b) to 13(d).

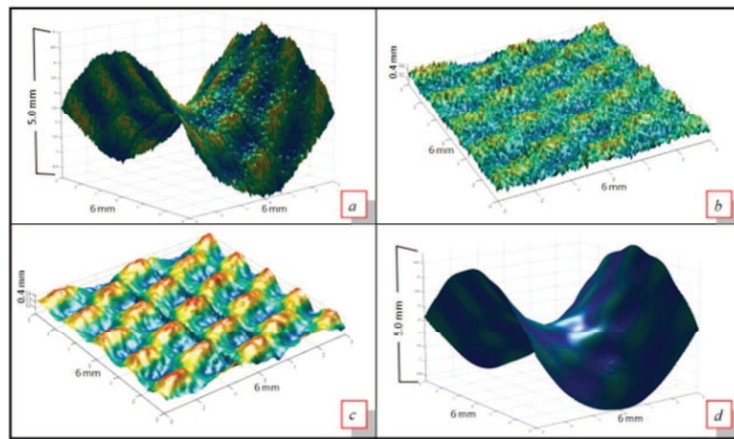


**Fig. 13:** Decomposition results of a saddle-shaped surface using curvature relaxation scheme using 32 decomposition levels: (a) The original textured surface; (b) roughness surface (the short-scale surface); (c) wavy surface (the middle-scale surface); (d) form surface (the long-scale form surface).

In this example, 32 decomposition levels are used to filter the surface into different scales: short-scale, middle-scale and long-scale equivalent to roughness, waviness and form respectively. The short-scale surface, roughness, is obtained using only the details coefficients of the first two decomposition levels and setting all other details coefficients of all other levels to zero. Whereas, the middle-scale surface is obtained using the details coefficients from the 3<sup>rd</sup> to the 30<sup>th</sup> decomposition levels and setting all

the other details coefficients in the other decomposition levels to zero. Finally, the form surface is obtained using only the approximation output of the last decomposition levels.

The proposed algorithm has also been applied to the other simulated surfaces and the results shown in Figs.14 and 15 for the spherical and egg-box surfaces respectively. Fig.14 shows the results of decomposition the spherical surface into short-scale (roughness), middle-scale (waviness) and long-scale (form) surfaces. As in the previous example, 32 decomposition levels are used; the short-scale surface is resulted from considering only the details coefficients of the 1<sup>st</sup> and the 2<sup>nd</sup> levels, the middle-scale surface is resulted from the details coefficients from the 3<sup>rd</sup> to the 30<sup>th</sup> levels, and long-scale is the approximation output of the 32<sup>nd</sup> level.

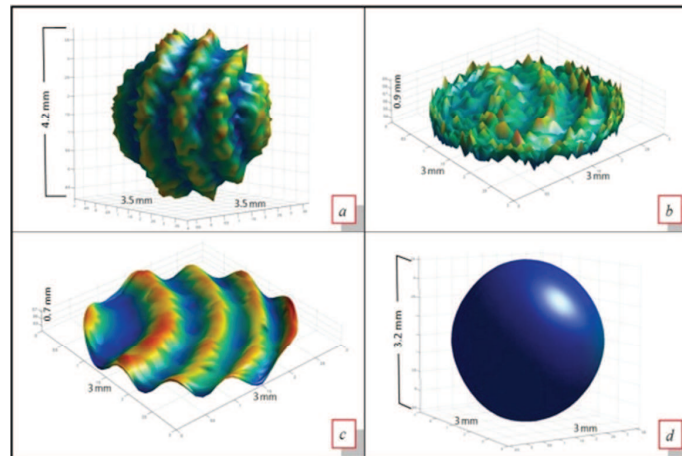


**Fig 14:** Decomposition results of a sphere surface using curvature relaxation scheme using 32 decomposition levels: (a) The original textured surface; (b) roughness surface (the short-scale surface); (c) wavy surface (the middle-scale surface); (d) form surface (the long-scale form surface).

Fig. 15 shows the results of decomposition the egg-box surface into short-scale (roughness), middle-scale (waviness) and long-scale (form) surfaces using the same filtering criteria as the above examples.

As shown in the examples above, the proposed algorithm successfully manages to decompose the computer generated freeform surface, represented by 3D triangular meshes, into different bands and scales. Computer generated meshes are more likely to be a regular or semi-regular type of meshes, So it is important to test the performance of the algorithm on real measured data meshes that are irregular in nature.

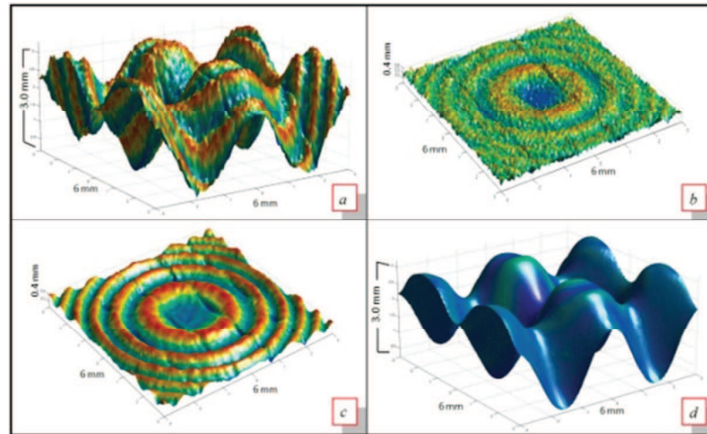


**Fig. 15:** Decomposition results of an egg-box surface using curvature relaxation scheme using 32 decomposition levels: (a) The original textured surface; (b) roughness surface (the short-scale surface); (c) wavy surface (the middle-scale surface); (d) form surface (the long-scale form surface).

## 6.2- Measured Surfaces

After the initial application of the proposed algorithm to computer generated freeform surfaces, the relaxation filtering scheme was performed on real surface measurement data. The data were obtained from coordinate measuring machine (CMM) measurement representing a portion of hip replacement components. Two surfaces were acquired from the CMM and represented by 3D triangular meshes; the first surface has 3380 vertices and 6591 faces, and second surface has 7182 vertices and 14108 faces (triangles) as shown in Table 2. These two measured surfaces are shown in Fig.16; we refer to these two surfaces as HipJoint-pt1 and HipJoint-pt2 as shown in Fig.16 (a) and (b) respectively.

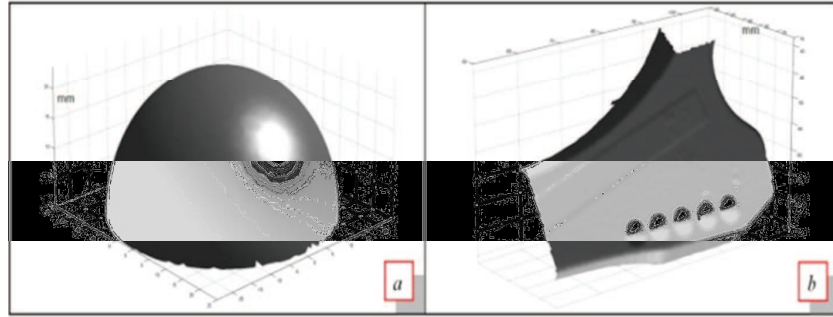


**Fig. 16:** Two real measured surfaces obtained with CMM for hip replacement components.

We refer to these surfaces as: (a) HipJoint-Pt1 and (b) HipJoint-Pt2.

**Table 2.** Mesh details of the real measured surfaces

Surface	Faces	Vertices
HipJoint-Pt1	6591	3380
HipJoint-Pt2	14108	7182

As with the computer generated surfaces, extra texture is imposed onto these surfaces to represent the short-scale and the middle-scale surfaces and then these surfaces are filtrated and decomposed using the proposed algorithm.

Figures 17 and 18 show the results of applying the proposed algorithm to decompose the HipJoint-Pt1 and HipJoint-Pt2 surfaces respectively into different scales. The original textured surfaces are shown in Figs. 17(a) and 18(a). As with the simulated surfaces, 32 decomposition levels are used to analyse the measured surfaces. The short-scale surfaces (roughness) are extracted using the details coefficients of the first and second levels and filtering out all other levels, the short-scale surfaces for HipJoint-Pt1 and HipJoint-Pt2 surfaces are shown in figures 17(b) and 18(b) respectively. The middle-scale surfaces (waviness) which resulted from only considering the details coefficients of the middle levels for the two measured surfaces are shown in figures 17(c) and 18(c). The long-scale surfaces (form) are shown in figures 17 (d) and 18(d). As mentioned earlier, the form surface is obtained by only

considering the output of the final approximation level and filtering out all the details coefficients of all other levels.

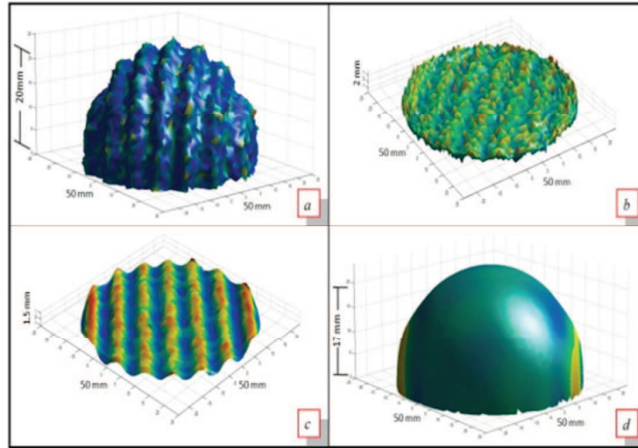


**Fig. 17:** Decomposition results of a HipJoint-Pt1 surface using curvature relaxation scheme using 32 decomposition levels: (a) The original textured surface; (b) roughness surface (the short-scale surface); (c) wavy surface (the middle-scale surface); (d) form surface (the long-scale form surface).

The above examples of the filtering and decomposing computer generated and real measured surfaces demonstrate that the proposed multi-scale relaxation algorithm is capable of filtering the texture of various types of freeform surfaces represented by regular or irregular 3D triangular meshes.

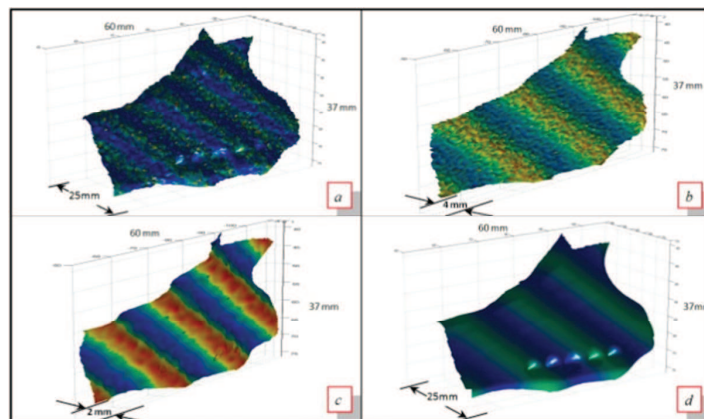


**Fig. 18:** Decomposition results of a HipJoint-Pt2 surface using curvature relaxation scheme using 32 decomposition levels: (a) The original textured surface; (b) roughness surface (the short-scale surface); (c) wavy surface (the middle-scale surface); (d) form surface (the long-scale form surface).



### 6.3- Comparisons with lifting based multi-resolution filtering algorithms.

The lifting wavelet transform is a powerful tool to analysis and to decompose various types of data into different scales and resolutions. It can be used to decompose regular as well as irregular data sets represented on grid or meshes.

Many researchers have proposed the use of the lifting schemes to analyse irregular data represented by meshes or graphs [16, 29-31]. Recently, the authors have also proposed a freeform filtering algorithm based on the lifting wavelets transform to filter freeform surfaces represented by 3D irregular meshes. Their algorithm can be briefly summarised in the following five steps, readers are advised to refer to the actual paper for full details of the algorithm [16]:

- 1- Split the surface data into even and odd.
- 2- Predict the odd vertices using the even vertices based on a mesh relaxation scheme.
- 3- Update the even vertices using the odd vertices.
- 4- Calculate the details for all odd vertices as the difference between the actual odd vertices and their predicted values (lifting details).
- 5- Remove all odd vertices using a mesh simplification algorithm to produce a coarser mesh (lifting approximations)

The main differences between lifting based algorithm and the proposed algorithms can be outlined in the following points:

- Firstly, the lifting based algorithm relaxes only the odd vertices and then calculates the details for odd vertices only; odd vertices cover around 30% of the total vertices in the mesh. The proposed algorithm, however, relaxed all vertices and then calculates the details for all vertices in the mesh. Calculating the details for all the vertices produce a smoother outcome at each approximation levels and therefore increases the filtering capabilities of the algorithm.
- Secondly, lifting based algorithm removes all the odd vertices from the fine mesh to produce the coarse mesh in a mesh simplification (down-sampling) step. This down-sampling is important to produce different levels of details, where the approximated mesh at each level

has fewer vertices and faces. Representing a mesh in different levels of details is important in the mesh visualisation, transmission and compression applications. The proposed algorithm does not perform any down-sampling procedure hence the approximated mesh has the same number of vertices and faces.

- Thirdly, the number of decomposition levels is limited in the lifting based algorithms due to the down-sampling step; more decomposition levels are still possible as long as the base mesh has not been reached. The base mesh is the coarsest mesh with only a few number of faces which cannot be simplified anymore. This is in contrast to the proposed algorithm where the number of decomposition levels is not limited and can be designed to suit the filtering application.
- Finally, the lifting based algorithm contains more operations and consumes more computational powers than the proposed algorithm.

The proposed technique is compared with the lifting based algorithm proposed recently by the authors [16] and the results are shown in Figs. 19-21.

Fig. 19 compares the filtering results of the computer generated spherical surface using the lifting based algorithm with the proposed techniques. The filtered forms, long-scale surfaces, using the lifting algorithm with 4, 16 and 24 decomposition levels are shown in Fig 19(a), 19(c) and 19(e) respectively. The long-scale surfaces resulted from the proposed algorithm using 4, 16 and 24 decomposition levels are shown in Fig 19(b), 19(d) and 19(f) respectively.

Figs.20 and 21 show the comparison results between the two algorithms for the real measured surfaces namely HipJoint-Pt1 and HipJoint-Pt2.

As shown in these figures, relaxation scheme produces smoother form results compared to the lifting based algorithm. Smoother form (long-scale) result means that the other short-scale and middle-scale surface components ( surface textured) are included in the details coefficients and isolated from the form which makes the decomposition of the surface into different scales easier and more accurate as have been shown previously in the paper.

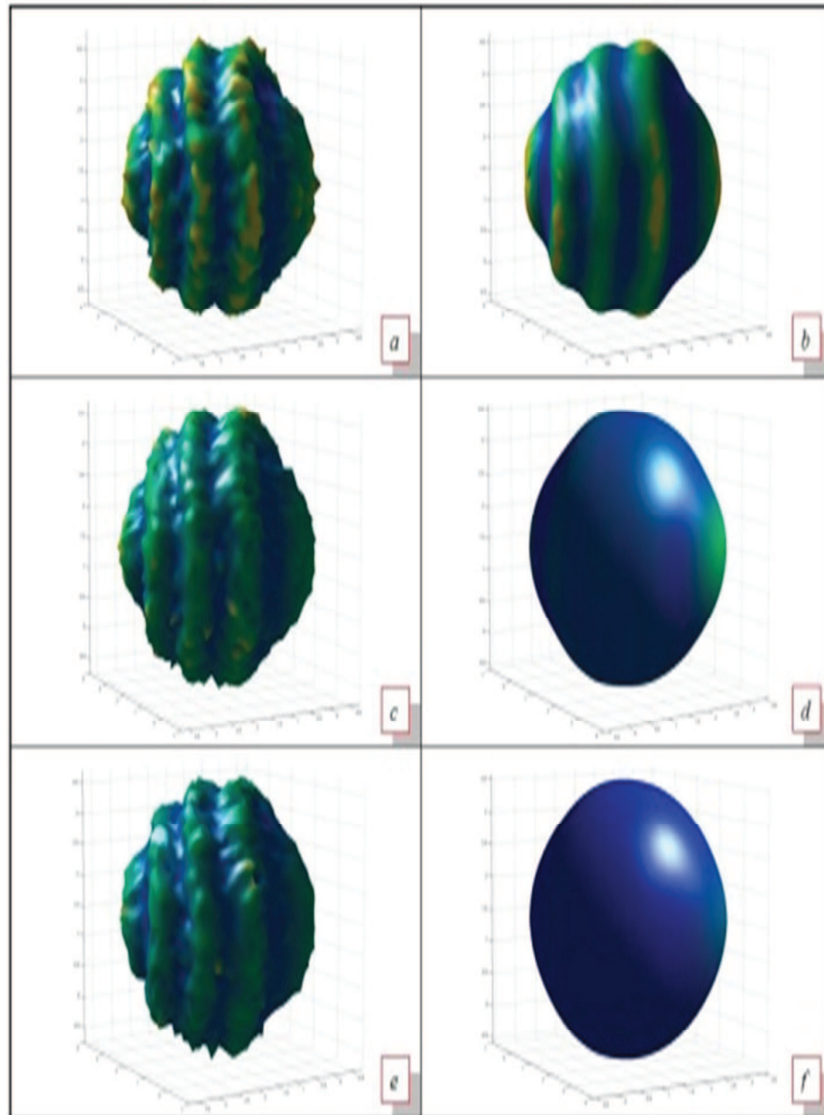


**Fig. 19:** Comparisons between lifting scheme and relaxation scheme filtering methods for the spherical surface: (a), (c) and (e) the results of lifting algorithm using 4, 16 and 24 decomposition levels respectively; (b), (d) and (f) the results of relaxation algorithm using 4, 16 and 24 decomposition levels respectively.

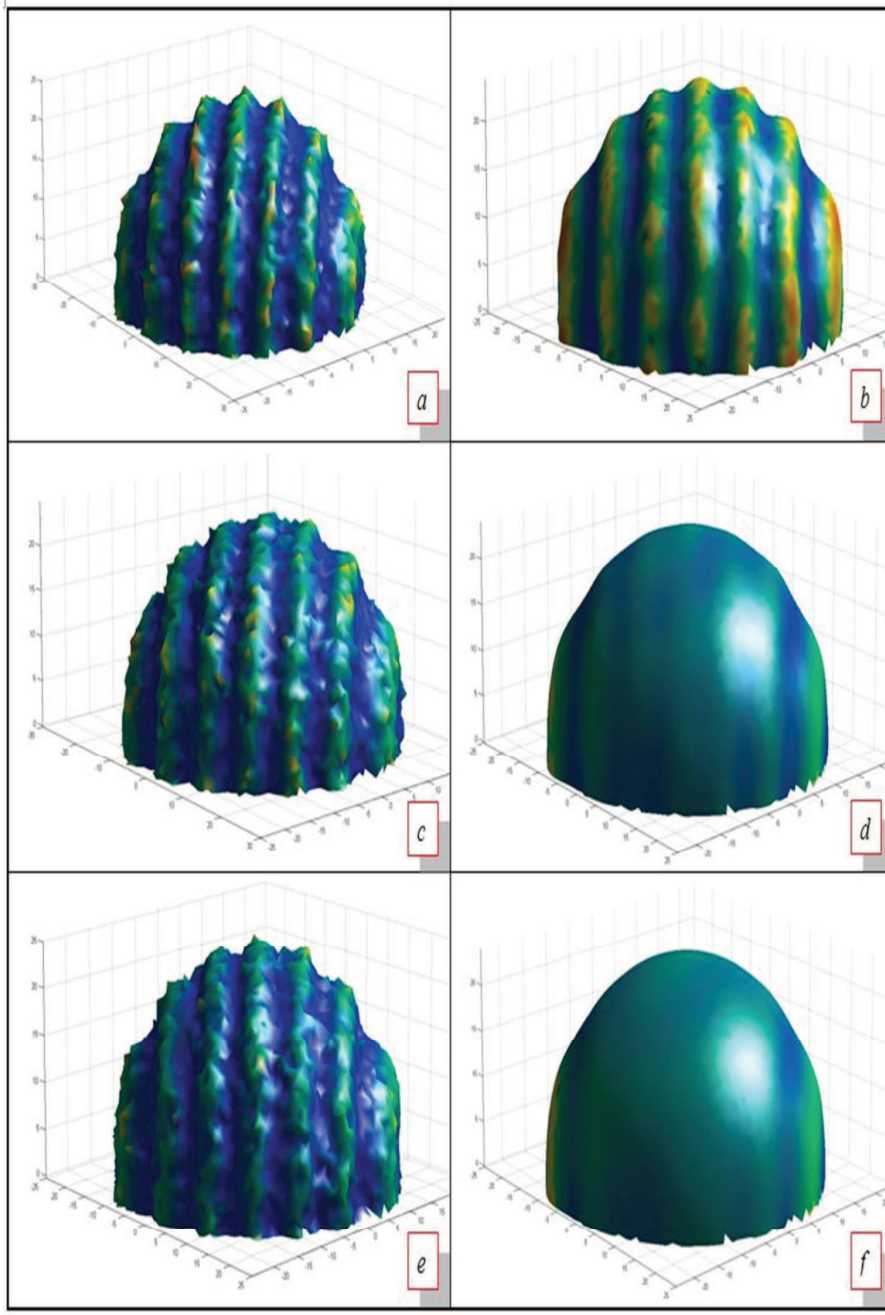


**Fig. 20:** Comparisons between lifting scheme and relaxation scheme filtering methods for the HipJoint-Pt1 surface: (a), (c) and (e) the results of lifting algorithm using 4, 16 and 24 decomposition levels respectively; (b), (d) and (f) the results of relaxation algorithm using 4, 16 and 24 decomposition levels respectively.

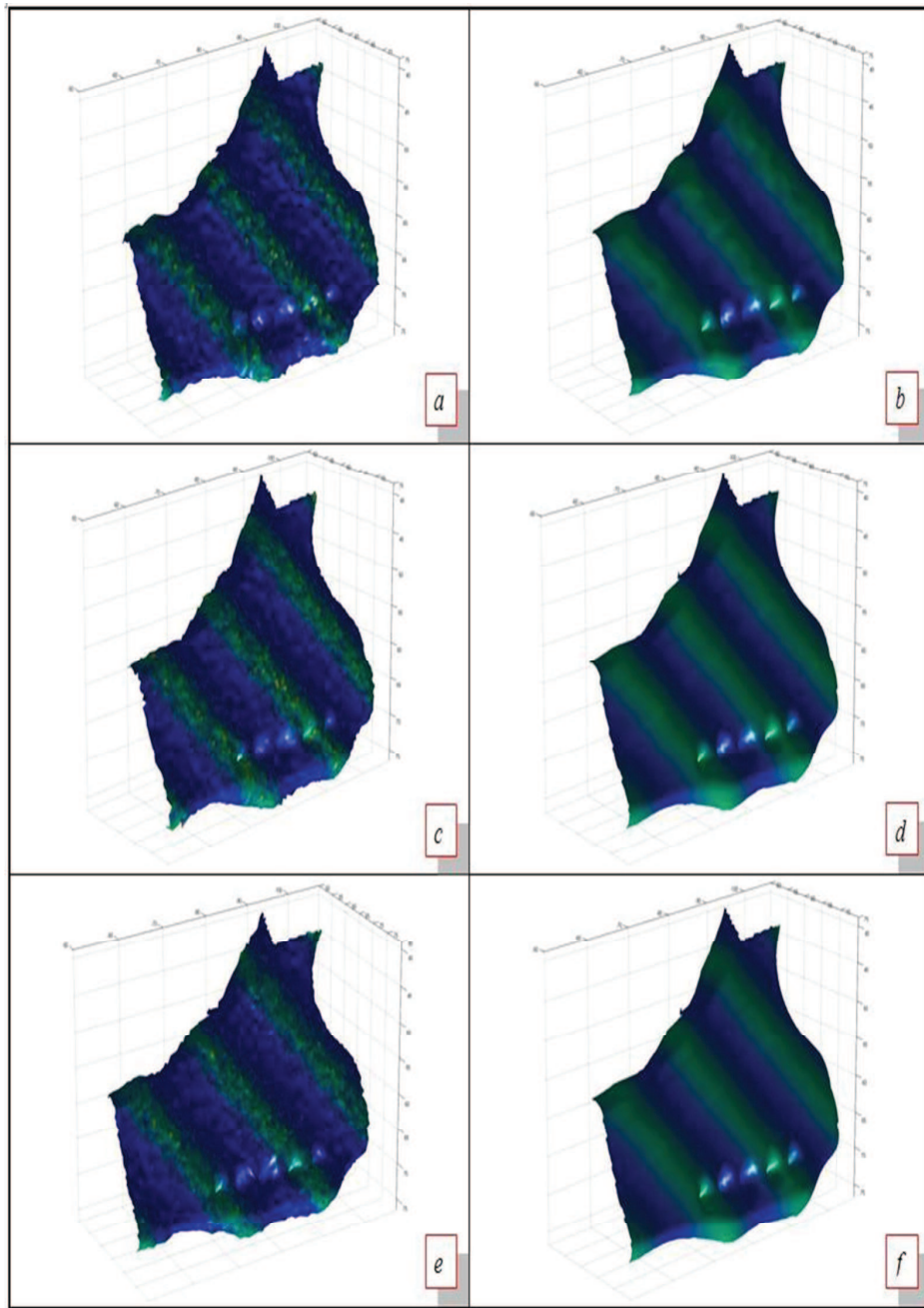


**Fig. 18:** Decomposition results of a HipJoint-Pt2 surface using curvature relaxation scheme using 32 decomposition levels: (a) The original textured surface; (b) roughness surface (the short-scale surface); (c) wavy surface (the middle-scale surface); (d) form surface (the long-scale form surface).

## **7- Conclusions and future work**

Freeform surfaces are rapidly emerging and being used in a wide range of fields, therefore it is crucial to have new techniques that are capable of filtering, decomposing and analysing these new surfaces. Throughout this paper, a new freeform filtering algorithm based on a mesh relaxation scheme has been proposed. The proposed technique has been applied successfully to filter both computer generated and measured freeform surfaces represented by 3D triangular meshes. Moreover, the results show that the proposed algorithm is also capable of decomposing freeform surfaces into different scales namely; the short-scale (roughness), the middle-scale (waviness) and the long-scale (form).

The decomposition is carried out by running a mesh relaxation algorithm iteratively. Each iteration results in decomposing the surface into an approximation and details. In the next iteration, the approximated surface is further decomposed into its approximation and details and so on. Extracting different surface scales is then performed by selecting different details levels and ignoring others as explained in the paper.

Furthermore, the proposed technique has been compared with a lifting based filtering algorithm. The comparisons show that the mesh relaxation algorithm produces a smoother filtered surface than the lifting based algorithm for the same number of the decomposition levels; this is because all surface vertices are being filtered in the mesh relaxation algorithm whereas only some selected vertices, odd vertices, are being processed in the lifting algorithm.

This paper is an initial investigation of freeform filtering using a mesh relaxation scheme and more future development is still needed. A key area of future research will be the investigation of different mesh relaxation schemes that could improve the filtering process and to study the advantages and disadvantages of each relaxation method. Gaussian filters have been successfully applied to filter Euclidean surface for decades and they have proven their utility in many different applications, therefore designing a Gaussian-like relaxation scheme, that calculates the relaxed value based on Gaussian weights, will be important to investigate. Furthermore, the proposed algorithm has only

been compared with a lifting wavelet algorithm; however it is important to compare this algorithm with other freeform filtering algorithms based on morphological or PDE in the future. Other area of interests will be the investigation of the relationship between the number of decomposition levels and the required cut-off wavelengths for roughness and waviness. Moreover it is important to investigate the effect of the mesh relaxation algorithm on the boundary vertices for open surfaces.

#### **Acknowledgement:**

The authors gratefully acknowledge the UK's Engineering and Physical Sciences Research Council (EPSRC) funding of the EPSRC Centre for Innovative Manufacturing in Advanced Metrology (Grant Ref: EP/I033424/1) and the European Research Council under its programme ERC-2008-AdG 228117-Surfund.

#### **References**

- [1] Whitehouse, D.J. Handbook of Surface and Nanometrology. Second Edition, CRC Press: Taylor and Francis Group, 2011 (ISBN 978-1-4200-8201-2).
- [2] Leach R. K. Fundamental Principles of Engineering Nanometrology. Elsevier, William Andrew, 2009 (ISBN 0080964540).
- [3] Blunt L., Jiang X. Advanced Techniques for Assessment Surface Topography: Development of a Basis for 3D surface Texture Standards "Surfstand". Butterworth-Heinemann, 2003 (ISBN 1903996112).
- [4] Jiang, X., Scott, P. J., Whitehouse, D. J. & Blunt, L. Paradigm Shifts in surface metrology. Part I, Historical philosophy. *Proc. R. Soc. A* **463**, 2007, pp: 2049–2070. (doi:10.1098/rspa.2007.1874)
- [5] Jiang, X., Scott, P. J., Whitehouse, D. J. & Blunt, L. Paradigm Shifts in surface metrology. Part II, The current shift. *Proc. R. Soc. A* **463**, 2007, pp: 2071–2099. (doi:10.1098/rspa.2007.1873)
- [6] Whitehouse, D. Surfaces and their Measurement. *Hermes Penton Ltd*, 2002.

- [7] ISO 11562: 1996 Geometric product specification (GPS) Surface Texture: profile method metrological characteristics of phase correct filters, 1996.
- [8] ISO 16610-21: 2011 Geometrical product specifications (GPS) - Filtration - Part 21: Linear profile filters: Gaussian filters, 2011.
- [9] ISO/CD 16610-61: 2010 Geometrical product specifications (GPS) - Filtration - Part 61: Linear areal filters: Gaussian Filters, 2010.
- [10] ISO/TS 16610-31: 2010 Geometrical Product Specification (GPS) – Filtration, 2010.
- [11] ISO 25178-2: 2012, Geometrical Product Specification (GPS) - Surface Texture: Areal - Part 2: Terms, definitions and surface texture parameters, 2012.
- [12] LeGoic G., Brown C.A., Favreliere H., Samper S. and Formosa F. Outlier filtering: a new method for improving the quality of surface measurements, *Meas. Sci. Technol.* 24 doi:10.1088/0957-0233/24/1/015001. (2012)
- [13] Formosa F., Samper S. and Perpoli I. Modal expression of form defects. *Proc. 9th CIRP Seminar on Models for Computer Aided Tolerancing (2005)*, pp. 1–9.
- [14] Jiang, X., Cooper, P. & Scott, P. J. Freeform surface filtering using the diffusion equation. *Proc R. Soc A*, Vol. **467**, Issue. **2127**, 2011, pp. 841–859. (DOI: 10.1098/rspa.2010.0307).
- [15] Jiang, X., Lou S. & Scott, P. J. Morphological method for surface metrology and dimensional metrology based on the alpha shape. *Meas. Sci. Technol.* Vol. **23** (2012) 015003 (9pp) (doi:10.1088/0957-0233/23/1/015003)
- [16] Abdul-Rahman H. S., Jiang, X. & Scott P. J. Freeform Surface Filtering Using the Lifting wavelet Transform. *Precision Engineering* Vol. 37, Issue. 1, January (2013), pp.187-202. (DOI: 10.1016/j.precisioneng.2012.08.002)
- [17] Kuhnel W. *Differential Geometry: Curves-Surfaces-Manifolds*. Second Edition, American mathematical society, 2005 (ISBN 0821839888).



- [18]Hubeli, A. & Gross, M. A survey of surface representations for geometric modelling. *Technical Report 335, ETH Zurich*, 2000, *Computer Science Department*.
- [19]Prautzsch, H., Boehm W. and Paluszny M. Bezier and B-Spline Techniques. Springer-verlag Berlin Heidelberg New York, 2002 (ISBN 3540437614).
- [20]Zhang X. Free-form surface fitting for precision coordinate metrology. PhD thesis, University of Huddersfield, (2009).
- [21]Guskov, I., Sweldens, W. & Schroder, P. Multiresolution signal processing for meshes. *Proceedings of ACM SIGGRAPH*, 1999, pp. 325–334.
- [22]Sweldens, W. The Lifting Scheme: A New Philosophy in Biorthogonal Wavelets Reconstructions. *Wavelet applications in signal and image processing III*, 1995, pp. 68-79.
- [23]Sweldens, W. Wavelets and the Lifting Scheme: A 5 Minute Tour. *Z. Angew. Math. Mech* vol. **76**, no. **2**, 1996, pp. 4-7.
- [24]Sweldens, W. The lifting scheme: A construction of second generation wavelets. *SIAM Journal on Mathematical Analysis*, vol. 29, no. 2, 1998 , pp. 511-546.
- [25] Eck, M., DeRose, T., Duchamp, T., Hoppe, H., Lounsbery, M. & Stuetzle, W. Multiresolution Analysis of Arbitrary Meshes. In *SIGGRAPH 95 Conference Proceedings, ACM SIGGRAPH, Addison Wesley, Reading, MA*, 1995, pp. 173–182.
- [26]Lounsbery, M., DeRose, T. & Warren, J. Multi-resolution Analysis for Surfaces of Arbitrary Topological Type. *ACM Transactions on Graphics*, Vol. **16**, No. **1**, 1997 ,pp. 34-73.
- [27]Bonneau, G. P. Multiresolution analysis on irregular surface meshes. *IEEE Transactions on Visualization and Computer Graphics* vol. **4**(4), 1998, pp. 365–378.
- [28]Daubechies, I., Guskov, I., Schroder, P. & Sweldens, W. Wavelets on Irregular Point Sets. *Phil. Trans. R. Soc. Lond. A*, **357**, 1999 ,pp.2387-2413.

- [29] Roy, M., Foufou, S., Koschan, A., Truchetet, F. & Abidi, M. Multiresolution Analysis for Meshes with Appearance Attributes. *Proc. IEEE on Image Processing ICIP2005*, vol. **III**, 2005, pp. 816-819.
- [30] Jansen, M., Nason, G. P. & Silverman, B. W. Multiscale methods for data on graphs and irregular multidimensional situations. *Journal of the Royal Statistical Society*, vol. 71, no. 1, 2009, pp. 97-125.
- [31] Narang, S. K. & Ortega, A. Lifting based wavelet transforms on graphs. *APSIPA ASC' 09*, 2009.
- [32] Schroder, P. & Sweldens, W. Spherical Wavelets: Texture Processing. In P. Hanrahan and W. Purgathofer, editors, *Rendering Techniques 95*, Springer Verlag, New York, August, 1995.
- [33] Schroder, P. & Sweldens, W. Spherical Wavelets: Efficiently Representing Functions on the Sphere. In *EGRW 95*, 1995, pp. 252-263.
- [34] Desbrun, M., Meyer, M., Schröder, P., & Barr, A., Implicit fairing of irregular meshes using diffusion and curvature flow. *Proceedings of ACM SIGGRAPH*, 1999, pp. 317-324.
- [35] Meyer, M., Desbrun, M., Schröder, P., & Barr, A. Discrete differential-geometry operators for triangulated 2-manifolds. *Proceedings of Visualization and Mathematics*, 2002.
- [36] Szczesna, A. The multiresolution analysis of triangle surface meshes with lifting scheme. in *Proceedings of MIRAGE Conference on Computer Vision/Computer Graphics Collaboration Techniques*, 2007.
- [37] Szczesna, A. Designing lifting scheme for second generation wavelet-based multiresolution processing of irregular surface meshes. *Proceedings of Computer Graphics and Visualization*, 2008.
- [38] Valette, S. & Prost, R. Wavelet-based multiresolution analysis of irregular surface meshes. *IEEE Transactions on Visualization and Computer Graphics*, vol. **10**, no. 2, 2004, pp. 113-122.
- [39] Roy, M., Foufou, S. & Truchetet, F. Recent Advances in Multiresolution Analysis of 3D Meshes and their Applications. *Proc. SPIE wavelet applications in industrial processing VII*, (2010), **Vol.** 7535, 75350H. (<http://dx.doi.org/10.1117/12.845595>)

- [40] Roy, M., Fofou, S., Koschan, A., Truchetet, F. & Abidi, M. Multiresolution Analysis for Irregular Meshes. *Proc. SPIE wavelet applications in industrial processing*, (2004), **Vol.** 5266, pp. 249-259, Providence, RI. (<http://dx.doi.org/10.1117/12.515974>)
- [41] Schneider, R. & Kobbelt, L. Geometric fairing of irregular meshes for freeform surface design. *Computer Aided Geometric Design*, **Vol.** 18, no. 4, pp. 359-379, (2001).
- [42] Hubeli, A. & Gross, M. Multiresolution methods for non-manifold models. *IEEE Transactions on Visualization and computer Graphics*, **Vol.** 7, no. 3, pp. 207-221, (2001).
- [43] Jiang X. J. and Whitehouse D. J. Technological shifts in surface metrology. *CIRP Annals - Manufacturing Technology*, (2012). (<http://dx.doi.org/10.1016/j.cirp.2012.05.009>)